Technoscience Journal for Community Development in Africa 5:1 (2026) 49–58
ISSN 2659-0573

Research Article

Optical, morphological, and structural properties of green-synthesized zinc oxide nanoparticles as a promising nanomaterial for integration in solar cells

Sunday Wilson Balogun, Sefiu Adekunle Bello, Akeem Sodiq Olalekan

Department of Materials Science and Engineering, Kwara State University Malete, Nigeria.

Abstract: Green - synthesized method for the production of metal oxide nanoparticle for energy conversion has received attraction over physical and chemical routes of synthesis due to its eco-friendliness, energy efficiency, and nontoxicity. Nanotechnology promotes large-scale production of materials for energy conversion, electronics, and optoelectronics. Research on biosynthesis of nanoparticles remains an inexhaustible field. This paper presents bio-synthesis of zinc oxide nanoparticle (ZnONPs) for integration in solar cells from Zinc nitrate hexahydrate using *Moringa oleifera* extract as capping and reducing agent. Analyses of zinc oxide nanoparticles' structural, optical, surface morphological, elemental composition, and chemical bond properties were conducted. The SEM analysis indicate a spherical, nanosized grain morphology with a diameter of 36.25 nm. The XRD analysis yielded an average crystallite size diameter of approximately 36.28 nm. XRD result revealed the wurtzite hexagonal nature of ZnO and showed that temperature annealing affects crystallite grain size. FT-IR spectroscopy confirmed formation of zinc oxide nanoparticles. Optical spectroscopic analysis showed that ZnO nanoparticles properties were influenced by temperature annealing. The band gap varies from 1.1 eV to 1.22 eV, which decreases with increase in annealing temperature. These findings elucidate the potential of extract from *Moringa oleifera* plant as a green source of capping agent for ZnO-NPs synthesis. The study establishes *Moringa oleifera* leaf extract as an efficient, eco-friendly precursor for ZnO NP synthesis. The results, also demonstrated the possibility of thermal annealing as a means of tunning ZnO nanoparticles properties. Overall, the potential embedded in these results suggest ZnO nanoparticles as a promising suitable nanomaterial for solar cell photo-anodes.

Key words: ZnO nanoparticles; *Moringa oleifera* extract; spin-coating; X-ray diffraction; Temperature annealing

1. Introduction

Metal oxides ion such as zinc oxide (ZnO) and titanium dioxide (TiO2) have been the subject of extensive research as a result of their rare physical and chemical properties. Zinc oxide an inorganic n-type semiconductor member with a direct bandgap between 3.3 eV and 3.7 eV at ambient temperature. ZnO has been extensively studied for optoelectronic, light-emitting devices, solar cells, dye-sensitized solar cells, biomedical applications, and electronic device technologies (Hadis and Umit, 2009). Zinc oxide is an inorganic oxide that is low-cost, non-toxic, and chemically stable, exhibits high photocatalytic activity, and has high electron mobility compared with titanium dioxide (Virkki et al., 2018; Zhang et al., 2009). Zinc oxide's uniqueness is based on its high coupling coefficient, high photo-stability, and its absorption of energy over a wide range of wavelength in the solar spectrum which is responsible for its choice for photonic and optoelectronic devices. Published research on nanoparticles synthesis using *moringa oleifera* leaf water extract precursor as nanomaterials have not been exhausted and exploited (Anta et al., 2012,). Previous authors mentioned the bioactive components present in *moringa oleifera* leaves such as vitamins, flavonoids, phenolic acid, and glucosides (Nama, 2016; Kalappurayil. 2016; Ghazali & Mohammed., 2011; Manguro et al. (2007). *Moringa oleifera* leaves also contain mineral elements such as Mg, K, Ca, P, and S as indicated by (Ngom et al., 2020; Bassey et al., 2018; Taylor et al.2007). Studies on zinc oxide nanoparticles have been widely focused on antibacterial, antifungal,

* Corresponding author:
Email: sunday.balogun@kwasu.edu.ng

KWASU PRESS AND PUBLISHING

bio-medicine, and for delivery design, to mention but a few rather than its exploration for energy applications (Kennedy et al; 2014, Gade et al., 2010; Fan et al., 2010; Wang 2008; Minegish et al., 1997). ZnO nanoparticle methods of deposition include spin-coating (Balogun et al., 2026; Balogun et al., 2020), sol-gel (Zahra et al., 2022; Dulta et al., 2021). Assisted combustion (Udayabhanu et al., 2019), spray pyrolysis (Bedia et al., 2015), Irradiation (Antipov et al., 2016), microwave-assisted processing (Ider et al., 2017), solvo-tthermal (Jamil et al;2014), ultrasonic assisted processing (Manjamadha et al., 2016), plasma-enhanced chemical vapor deposition (Liu et al., 2004), laser-assisted chemical deposition (Guan et al., 2008), sono-chemical (Xu et al., 2013), hydrothermal (Aneesh et al., 2007), wet polymerization (Hong et al., 2006), thermal decomposition (Salavati-Niasari et al., 2008; Baskoutas et al., 2007), precipitation (Ghorbani et al., 2015), microemulsion (Eslamian and Shekarriz, 2009), and lyophilization (Ngom et al., 2016). Technologies for the synthesis of nanoparticles is broadly divided into three methods: physical, chemical, and biosynthesis. Physical and chemical methods are energy-consuming, expensive, toxic, and hazardous due to chemical use polluting and leading to environmental degradation (Isnaeni et al., 2021; Pushpamalini et al., 2020; Sharmila et al., 2018). However, biosynthesis has relative advantages over another method of synthesis; such advantages are ease of fabrication, environmental friendliness, being less hazardous, and non-toxicity. Ngom et al. (2020) reported NiO and ZnO nanoparticles synthesis by *Moringa oleifera* leaf extract with zinc nitrate hexahydrate as a precursor. NiO NPs and ZnO NPs average crystallite sizes were 17.80 and 10.81 nm, with band gaps of 4.28 eV and 3.35 eV, respectively. Saka et al. (2021) reported use of *moringa* extract to produce nanoparticle with zinc nitrate hexahydrate as a precursor. They observed a wide band gap at 350 nm in the visible region of the solar spectrum and high-purity nanoparticles. Pal et al. (2018) investigated photocatalytic and antibacterial properties of biosynthesized ZnO nanoparticles via *moringa Oleifera* extract. They reported a hexagonal wurtzite structure nanoparticles with grain size of 52 nm. Gonzalez-Fernandez et al. (2021) utilized *moringa oleifera* extract as a capping and reducing agent to produce ZnO nanoparticles. They presented a result indicating 47.2 nm spherical nanosized diameter material and 25 nm grain size diameter with the FE-SEM technique. Photocatalytic properties of ZnO nanoparticles produced via *moringa Oleifera* extract was evaluated by Adam et al. (2021) after thermal annealing at a temperature range of 300 to 500 °C. The reported result showed the absorption band at 422-497 cm $^{-1}$ for FTIR with Zn-O stretching and O-H bond at 3417 cm $^{-1}$ absorption peak. Furthermore, an increase in electron properties and bond formation was achieved as the temperature increased, and at 500 ºC, methylene blue degradation was experienced. Irfan et al. (2021) used *moringa oleifera* gum to synthesize silver and zinc oxide nanoparticles against multidrug-resistant bacteria. This study examines and reports the synthesis of zinc oxide nanoparticles using the *moringa oleifera* leaf extract. Our study covers optical, morphological, Fourier transform-infrared analysis, structural, and elemental composition of synthesized zinc oxide nanoparticles and the results reported.

2. Materials and methods

2.1. Materials

Zinc nitrate hexahydrate, used as a precursor, was purchased from Sigma-Aldrich. Reagents and other chemicals such as ethanol and sodium hydroxide (NaOH) were purchased from Lab Trade Scientific and Chemical Stores, a reputable vendor in Ilorin, Kwara State, Nigeria. Leaves of *Moringa oleifera* tree were harvested from the corresponding author's farm.

2.2. Preparation of Moringa Oleifera water extract

Harvested *Moringa Oleifera* leaves were washed with tap water and distilled water to remove dirt and then air-dried for 15 days at ambient temperature. A mass of 5.0 g of dried moringa *oleifera* was heated in 50 ml of distilled water to extract the bioactive nutrients, using a magnetic stirrer set at 70 ºC for 1 hour. After cooling, the solution was filtered through Whatman filter paper to remove residues and stored.

2.3. Synthesis of ZnONPs using water extract Moringa Oleifera

Zinc oxide nanoparticles (ZnONPs) were synthesized via a green route employing *Moringa oleifera* extract (L- ascorbic acid, $C_6H_8O_6$) as a bio-reductant. *Moringa Oleifera* aqueous extract is to reduce zinc precursors to ZnO nanoparticles. 0.2 g of zinc nitrate hexahydrate was dissolved in 25 mL of ethanol and stirred continuously for 3 h to obtain a zinc nitrate hexahydrate solution. Subsequently, 10 mL of *Moringa oleifera* extract was introduced into a 0.7 M zinc nitrate hexahydrate aqueous solution and stirred at ambient temperature for 3 h without heat treatment. In parallel, a 0.7 M

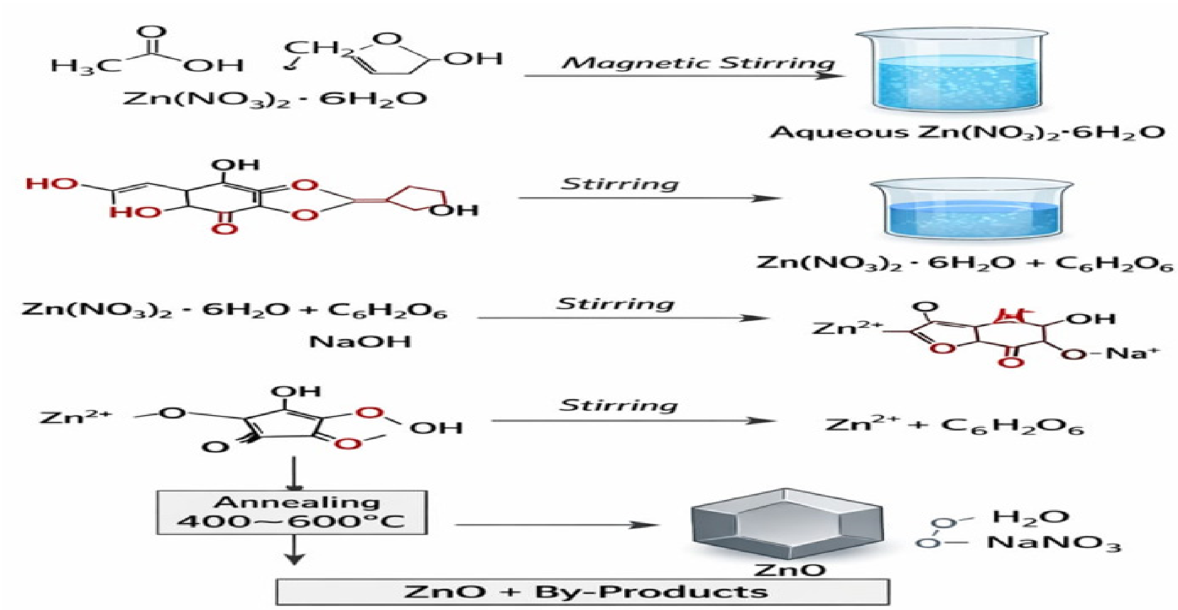

(a) Graphical reaction scheme

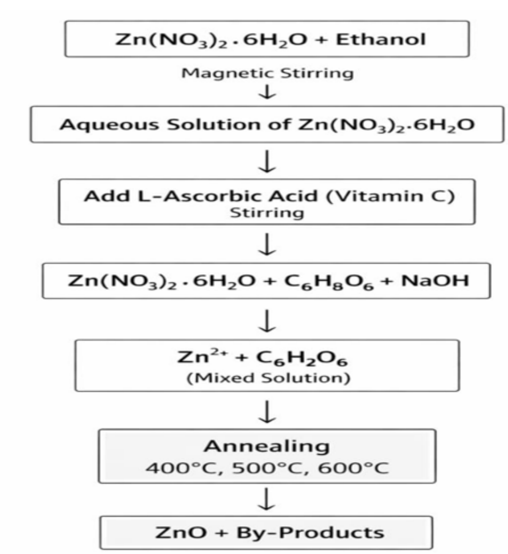

(b) Flow chart

Fig.1: Summarized green synthesis process of ZnO nanoparticles (a) Graphical reaction scheme (b) Flow chart.

aqueous ethanol solution was prepared, mixed with sodium hydroxide (NaOH), and stirred thoroughly. The two solutions were combined and stirred for an additional 3 h to promote nanoparticle formation.The resulting slurry of $Zn(OH)_2$ was separated by removing excess fluid, washed repeatedly with distilled water and acetone to eliminate residual impurities, and dried in an oven (Uniscope SM 9053, Surgifriend Medicals, England) at 100 °C for 1 h. The dried light-brown product was pulverized using a mortar and pestle, then divided into three portions. Each portion was annealed in a Carbolite tubular furnace (model SRW 21-501042, type CT17) at 400 °C, 500 °C, and 600 °C for 1 h 30 min, respectively, yielding a white ZnO nanopowder. The annealed powders were subsequently ground and sieved to obtain nanoscale particles suitable for characterization which in consistent with previous reports, nanoparticle formation was confirmed at annealing temperatures ≥400 °C (Jayachandran et al., 2021; Jafarirad et al., 2016). The process of synthesis is shown in figure 1 (a and b)

2.4. *Material Characterization of the zinc-based nanoparticles*

Spectroscopic optical properties were observed with a spectrometer (model ASpect UV-1.4.0.8031, Analytik Jena AG) and recorded in the wavelength 250.00–700.00 nm. FTIR spectroscopy (BUK model M530) recorded the functional group, chemical bond, and absorption band. The crystal structure and the size of the grain were determined from the analysis of XRD (ASC6-PM) with Cu Kα (λ=15405 Ǻ). Zinc oxide nanoparticles surface morphology was recorded with scanning electron microscopy (JOEL-JSM 7600F) and Electron dispersive X-ray revealed elemental composition of nanoparticles synthesized.

3. Results and discussion

3.1. *FTIR Spectroscope analysis*

FT-IR spectra pattern of ZnONPs annealed at (a) 400 ºC, (b) 500 ºC and (c) 600ºC is illustrated in figure 2. For

ZnONPs annealed at 400º C: Spectroscopic absorption bands observed at 3303.99 cm $^{-1}$, 2918.09 cm $^{-1}$, and 2849.84 cm $^{-1}$ indicates hydrogen single bond OH stretch which is related to both symmetric and asymmetric stretching mode of the hydroxyl functional group (Zn-OH). Absorption peak at wavenumber 1652.57 cm $^{-1}$ indicate N-H bend in double bond region of C=C, C=O and C=N. Absorption peaks at wavenumber 1413.37 cm $^{-1}$, 1316.33 cm $^{-1}$, 1056.50 cm $^{-1}$, and 647.52 cm $^{-1}$ fall under finger print region. The peak at 1413.37 cm $^{-1}$ indicates carboxylate, C-O symmetric stretching mode which possibly came from reactive carbon during the process of synthesis. Zn –OH functional group appeared at wavenumber of 1413.37 cm $^{-1}$, 1316.33 cm $^{-1}$, 1056.50 cm $^{-1}$, and 647.52 cm $^{-1}$ is assigned to Zn-O stretching and Zn-O-Zn bridging stretching vibrations modes.

FTIR Spectroscope analysis of ZnONPs annealed at 500º C: the absorption band observed at a high wavenumber of 3674.65 cm $^{-1}$ shows the compound contains an oxygen - related group, such as alcohol or Phenol. Wavenumber of 3434.44 cm $^{-1}$ is attributed to hydroxy functional group, H-bonded O-H stretch, the absorption band at a wave number of 3021.54 cm $^{-1}$ is assigned to Olefinic (alkene) C-H stretch or trans-C-H stretch. 2898.29 cm $^{-1}$ indicates methyne C-H stretch linear aliphatic compounds corresponding to symmetric and asymmetric modes (Coates, 2000; Nandiyanto et al; 2019). Wave number 2627.66 cm $^{-1}$, 2524.51 cm $^{-1}$, wavenumber of 2156.07 cm $^{-1}$ is assigned to thiocyanate (-SCN) functional group. Wavenumber of 1819.25 cm $^{-1}$ indicates carbonyl compound functional group (Aryl carbonate), Finger print region wavenumber of 1355.95 cm $^{-1}$ is assigned to Phenol or tertiary alcohol, OH bend. Zn –OH functional group appeared at wavenumber of 880.86 cm $^{-1}$ and 728.67 cm $^{-1}$. Zn-O stretching and Zn-O-Zn bridging stretching vibrations modes. These lower wavenumbers indicate ZnO material and stretching vibration of ZnO-NPs.

For ZnONPs annealed at 600º C: The spectroscopic absorption bands observed at 3460.05 cm $^{-1}$, 3021.29 cm $^{-1}$, 2897.89 cm $^{-1}$, 2627.67 cm $^{-1}$, 2524.14 cm $^{-1}$ indicates hydrogen single bond which is related to both symmetric and asymmetric stretching mode of the hydroxyl functional group (Zn-OH) (Nandiyanto et al; 2019). The hydroxyl stretching vibrations of O-H which occurred at wavenumber of 3460.05 cm $^{-1}$ showed the existence of water absorbed (Farrokhi et al; 2014). The absorption band peak at 3021.29 cm $^{-1}$ confirms the existence of a simple unsaturated olefinic compound. The appearance of C-H symmetric and asymmetric functional group bands at a wavenumber of 2897.89 cm $^{-1}$, 2627.67 cm $^{-1}$ and 2524.14 cm $^{-1}$ identified the existence of aliphatic compounds (Ngom et al.2020 ; Vafaee and Ghamsari ;2007). The absorption band peak observed at 1819.14 cm $^{-1}$ in the double bond region is assigned to the active carbonyl functional group. The peak at 1456.39 cm $^{-1}$ indicates carboxylate, C-O symmetric stretching mode which possibly arises from reactive carbon during the process of synthesis (Ngom et al. 2020; Xiong et al; 2006; Hiaing et al; 2005). Zn –OH functional group appeared at wavenumber of 877.52 cm $^{-1}$, 728.95 cm $^{-1}$ and 679.29 cm $^{-1}$ in the finger print region which is attributed to Zn-O stretching and Zn-O-Zn bridging stretching vibrations modes (Nandiyanto et al; 2019; Lu et al; 2012). The absorption peaks noticed at finger print region indicated formation of nanoparticles.

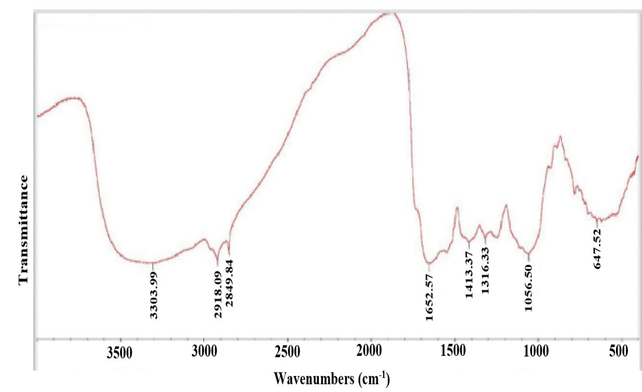

(a) 400º C

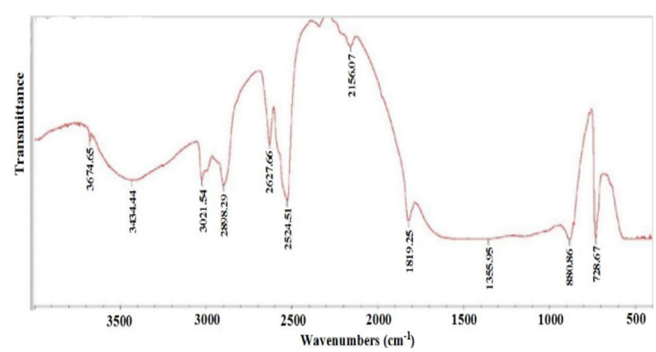

(b) 500º C

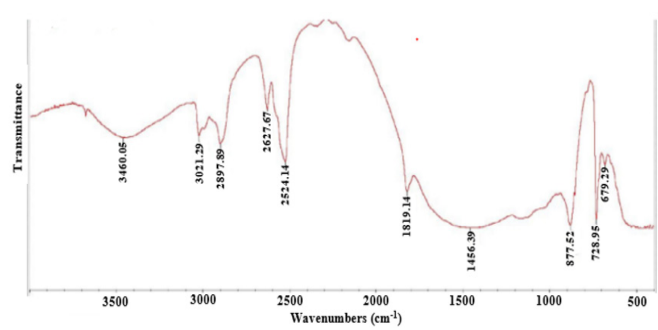

(c) 600º C

Fig.2 (a, b, c) FT-IR spectra pattern of (a) ZnONPs annealed at 400 ºC, (b) 500 ºC and (c) 600ºC

3.2. *X-ray Structural analysis*

Figure 3 (a, b and c) shows the XRD analysis structure at varying annealing temperatures 400 ºC, 500 ºC and 600 ºC. The XRD patterns miller indices identified as (100), (002), (101), (102), (110), (103), (200), (112), (201) consistent with the wurtzite hexagonal structure of ZnO. The planes of ZnO concur with Joint Committee on Powder Diffraction Standard (JCPDS) card number 01-079-0206. The dominant peak occurred at Bragg's angle (~ 32 º) at miller indices (100) for the varying annealing temperature of 500 ºC. Sharp peaks indicate a better purity and a better crystallinity nanoparticle. The Debby Scherrer's relation formula equation (1) was used to calculate the crystalline size of the nanoparticle.

$$\phi = \frac{0.94\lambda}{\Delta \cos\theta} \quad (1)$$

Where λ is the wave length of Cu-Kα radiation, ϕ is the crystallite size in nanometer (nm), Δ is the full width at half maximum of the peak in radian (rad) and θ is the Bragg diffraction angle in degree (º). The average size of the grain diameter calculated was approximately 36.28 nm which is similar with the range reported by (Gonzalez-Fernandez et al. 2021; Ngom et al. 2020).

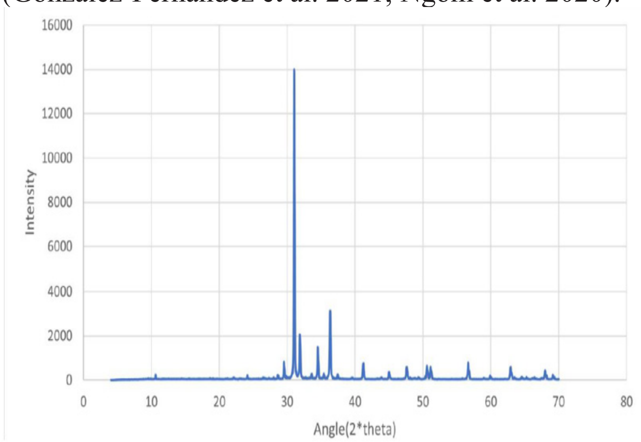

(a) 400 ºC

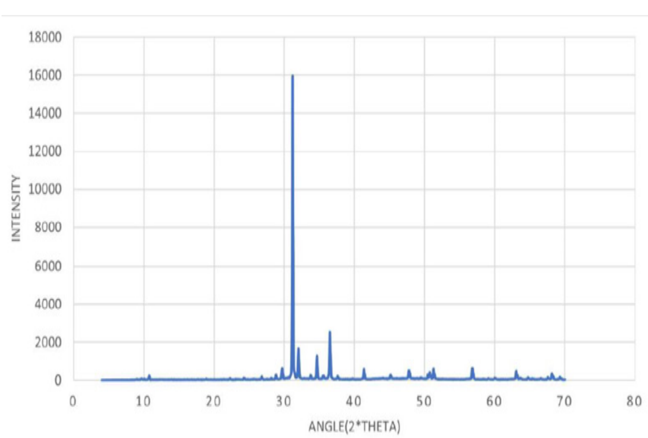

(b) 500 ºC

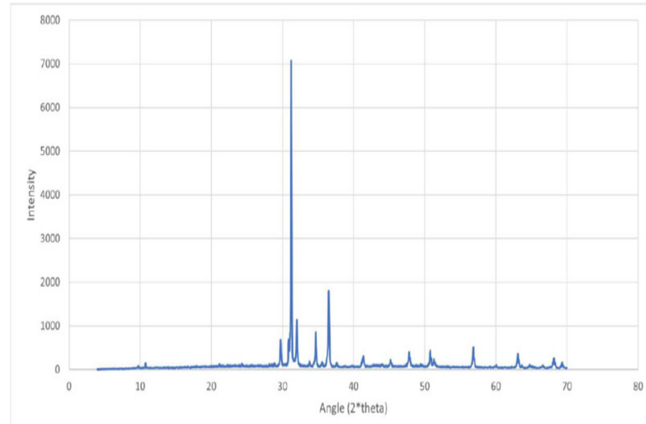

(c) 600 ºC

Fig. 3 (a, b and c) XRD pattern of ZnO-NPs annealed at (a) 400 ºC, (b) 500 ºC, and (c) 600 ºC

3.3. *SEM and EDX analyses*

3.3.1. *Effects of Temperature Annealing on ZnO Nanoparticles morphology*

Figure 4 (a, b, and c) show the morphological images of annealed ZnONPs thin film as recorded by Scanning Electron Microscope energy dispersive X-ray spectroscopy (SEM-EDS Phenom Prox model, manufactured by phenom World Eindhoven, Netherlands). The nature of the grain is spherical and granular. The size of the grain is estimated to be 36. 25 nm. The size of the grain increased with increasing annealing temperature which implies more absorption of photon energy, thereby increasing the energy conversion rate. The morphological image at 400 ºC is relatively agglomerated, as shown in Figure 4 (a). Figure 4 (b) shows finer and bigger grain sizes in comparism to Figure 4 (a), implying that ZnO nanoparticles parameters can be tuned by annealing temperature.

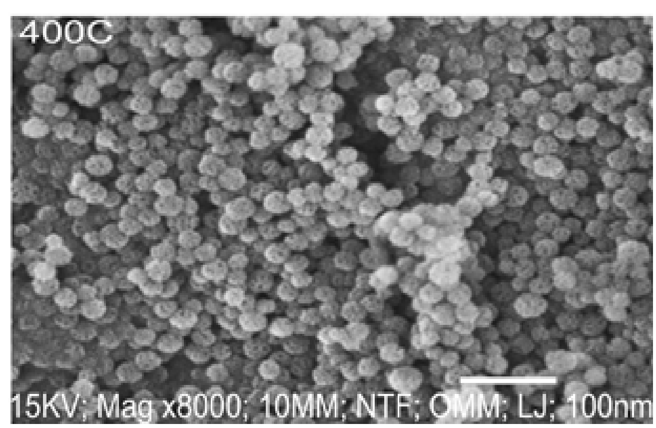

(a)

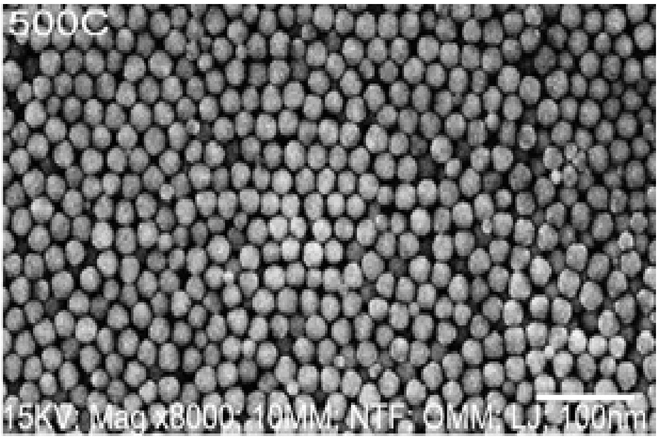

(b)

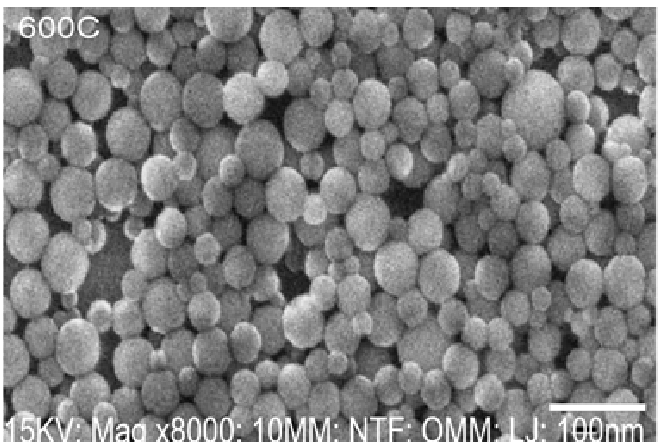

(c)

Fig.4 SEM images of ZnONPs at (a) 400 ºC, (b) 500 ºC and (c) 600 ºC

3.3.2. *Effects of Temperature Annealing on the Elemental Composition*

The Energy dispersion X-ray spectroscopy scans and provide information on elements present and atomic weight in percentage (%). Figure 5 (a, b, c) illustrate the elements and the weight percentage. Other elements present, such as carbon possibly arose from reactive carbon (bioactive compounds) during the synthesis process. *Moringa oleifera* leaves from the literature contain mineral elements such as Mg, K, Ca, P, and S (Ngom et al., 2020; Bassey et al., 2018; Taylor et al., 2007). Oxygen must have been trapped during the synthesis process (synthesis was done outside the glove box). The zinc atomic weight percentage increased with increasing annealing temperature. The elemental weight percentages of Zn and oxygen confirmed the formation of nanoparticles. The EDX analysis result agreed with the FTIR and XRD analytical results.

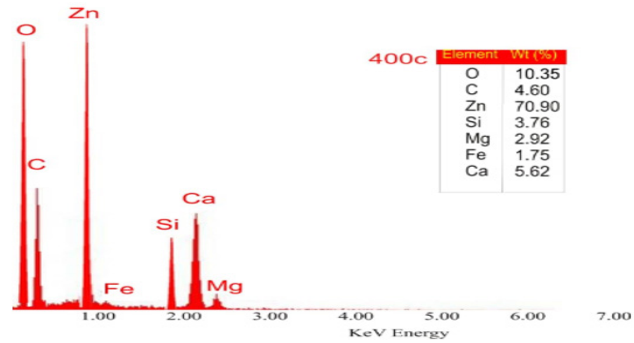

(a)

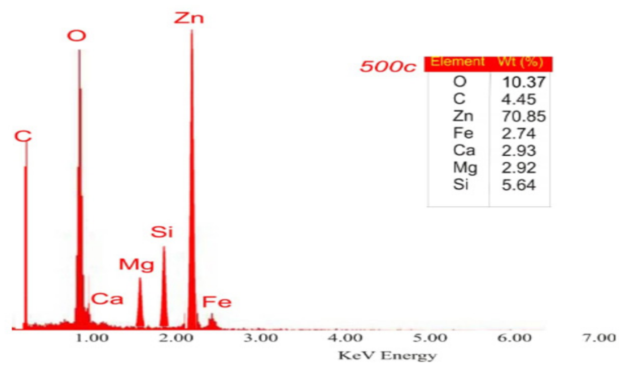

(b)

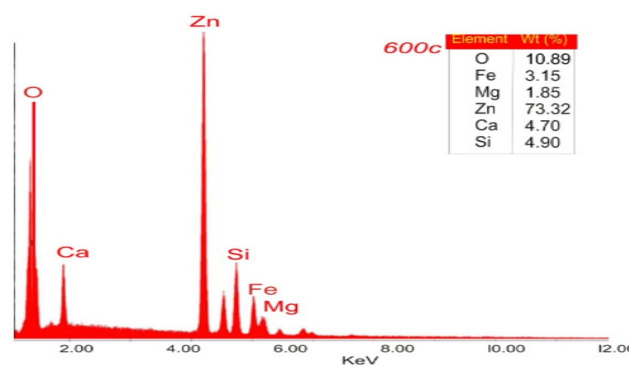

(c)

Fig. 5: Electron dispersive x- ray microscopy analysis of ZnONPs annealed at (a) 400 ºC, (b) 500 ºC and (c) 600ºC

3.4. *Optical Spectroscopic Analysis*

3.4.1 Effects of Temperature Annealing on ZnO Nanoparticle Thin Films

Figure 6 shows the optical UV-visible absorption spectra of zinc oxide nanoparticles annealed at 400 ºC, 500 ºC, and 600 ºC, respectively. The peak absorption occurred at a wavelength of 380 to 400 nm at 500 ºC. ZnO nanoparticles exhibited the highest excitation absorption at wavelengths of 380 to 400 nm.

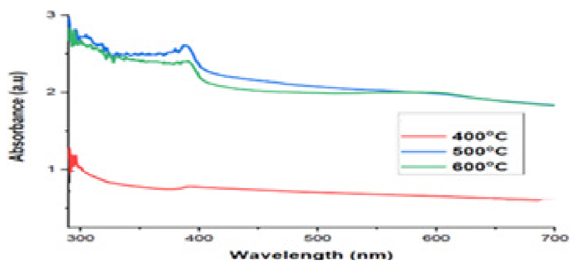

Fig. 6 UV- Visible absorption spectroscopy of ZnO nanoparticles

3.4.2. Determination of band gap

Figure 7 depicts graph of $(\alpha h\nu)^2$ versus hν for different annealing temperatures. The band gap was determined from the Tauc plot by extrapolating the linear portion of the $(\alpha h\nu)^2$ curve (Figure 8) against photon energy (hν) on the x-axis. The linear portion of the plot indicates the direct band-gap transition. The optical absorption coefficient (α) and photon energy (hν) are related by Equation (2) for the direct allowed quantum jump from the filled state of electrons to the empty conduction band.

$$(\alpha h\nu)^2 = A(h\nu - Eg) \tag{2}$$

where α is the absorption coefficient, *A* is a constant, *hν* is the photon energy, and Eg equation (3) is the band-gap in electron volt (eV).

$$Eg = \frac{hC}{\lambda}. \tag{3}$$

Where h is the Planck's constant = 6.62×10^{-34} J.S, C = 3×10^{8} m. s^{-1} is the velocity of light and λ is the wavelength in nanometer (nm). In our experiment, the band gap varied from 1.1eV to 1.22 eV, which is lower than the bulk value of approximately 3.37 eV. This reduction is attributed to crystal defects, non-stoichiometric phases due to oxygen vacancies, and internal stress (González-Fernández et al., 2021; Bindu and Thomas, 2017; Çağlar et al., 2009; Srikant and Clarke, 1998).

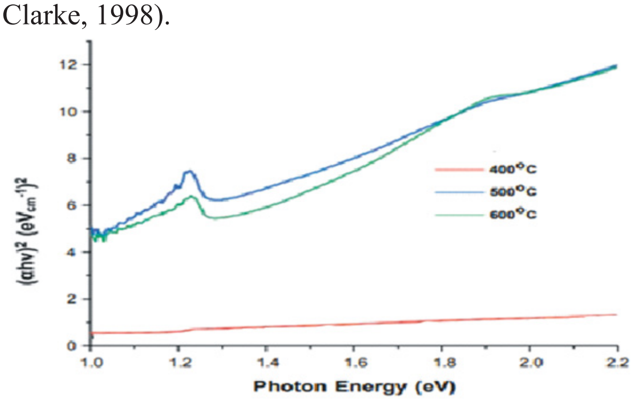

Fig. 7 Plot of $(\alpha h\nu)^2$ vs hν for different annealing temperature

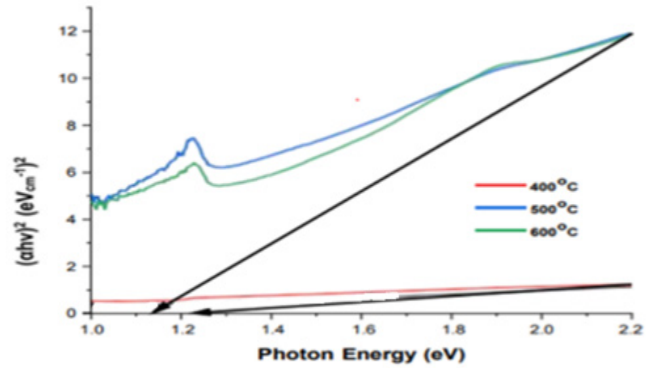

Fig. 8 Tauc plot of optical energy band gap of ZnO nanoparticle

4. Conclusion

Leaf extract of *Moringa oleifera* plant have been used to produce Zinc oxide nanoparticles and its properties evaluated as nanomaterials for sustainable renewable energy. Metal ions properties such as ZnO can be tuned by biosynthesis and annealing temperature. The results from FT-IR spectra and chemical bond analysis confirmed the formation of nanoparticles, and structural analysis revealed wurtzite hexagonal structure of ZnO. EDX analytical result agrees with the FTIR and XRD as per formation of nanoparticles. The combination of ZnO nanoparticle properties reveals their potential for application in sustainable renewable energy devices. The optical transmission of the films was influenced by annealing at different temperatures. The value of band gap varied from 1.1 eV to 1.22 eV. Further work is required and is ongoing to evaluate the electrical characteristics of Zinc oxide nanoparticles. Such work will evaluate the current-voltage characteristics to determine the resistivity, conductivity, long-term performance, and power conversion efficiency when integrated into solar cells as photo anode.

5. Funding

The research was not supported by any grant.

6. Competing interest

We the authors declare that we have no known competing interest.

7. Acknowledgments

The authors wish to express their gratitude to Materials Science & Engineering department, Kwara State University, Nigeria where the research was carried out.

References

Abel, S., Tesfaye, J. L., Nagaprasad, N., Shanmugam, R., Dwarampudi, L. P., & Krishnaraj, R. (2021) Synthesis and characterization of zinc oxide nanoparticles using Moringa leaf extract. *Journal of Nanomaterials*, 2021, 6 pages. https://doi.org/10.1155/2021/4525770

Adam, F., Himawan, A., Aswad, M., Ilyas, S., Heryanto, Anugrah, M. A., & Tahir, D. (2021) Green synthesis of zinc oxide nanoparticles using Moringa oleifera L. water extract and its photocatalytic evaluation. *Journal of Physics: Conference Series,* 1763, 012002. https://doi.org/10.1088/1742-6596/1763/1/012002

Aneesh, P. M., Vanaja, K. A., & Jayaraj, M. K. (2007) Synthesis of ZnO nanoparticles by the hydrothermal method. In Z. Gaburro & S. Cabrini (Eds.), *Nanophotonic Materials IV* (Vol. 6639, p. 66390J). SPIE. https://doi.org/10.1117/12.730364

Anta, J. A., Guillén, E., & Tena-Zaera, R. (2012) ZnO-based dye-sensitized solar cells. *Journal of Physical Chemistry C*, 116, 11413–11425. doi:10.1021/jp3010025

Antipov, A. A., Arakelian, S. M., Bukharov, D. N., Itina, T. E., Kutrovskaya, S. V., Kucherik, A. O., & Nogtev, D. S. (2016) Studying the synthesis of metal nanoparticles during laser irradiation of targets in liquid media. *Bulletin of the Russian Academy of Sciences: Physics*, 80(4), 351–357.

Balogun, S. W., Oladele, O. O., Sanusi, J. Y. K., & Olayinka, O. H. (2020) Green synthesis and characterization of zinc oxide nanoparticles using bashful (Mimosa pudica) leaf extract: a precursor for organic electronics applications. *SN Applied Sciences*, 2, 504. https://doi.org/10.1007/s42452-020-2127-3

Balogun, S. W., Oyeshola, O. H., Bello, S. A., Adewumi, H. K., & Sanusi, Y. K. (2026) Evaluation of environmentally friendly zinc oxide nanoparticles synthesized using Carica papaya leaf extract for renewable energy applications. *Iraqi Journal of Applied Physics*, 22(1), 131–136.

Baskoutas, S., Giabouranis, P., Yannopoulos, S. N., Dracopoulos, V., Toth, L., Chrissanthopoulos, A., & Bouropoulos, N. (2007) Preparation of ZnO nanoparticles by thermal decomposition of zinc alginate. *Thin Solid Films,* 515(24), 8461–8464.

Bassey, K., Semenya, A., Mabowe, M., Mabuza, M. (2018) South African Moringa oleifera Lam: a review of its phytochemistry, commercialization and quality control, *Int. J. Med. Plants Nat. Prod.* 4, 5–35. doi.org/10.20431/2454- 7999.0404002.

Bedia, A., Bedia, F. Z., Aillerie, M., Maloufi, N., & Benyoucef, B. (2015) Morphological and optical properties of ZnO thin films prepared by spray pyrolysis on glass substrates at various temperatures for integration in solar cells. *Energy Procedia*, 74, 529–538.

Bindu, P., & Thomas, S. (2017) Optical properties of ZnO nanoparticles synthesized from a polysaccharide and $ZnCl_2$. *Acta Physica Polonica* A, 131(6), 1474–1478. doi:10.12693/APhysPolA.131.1474

Çağlar, M., Ilican, S., & Çağlar, Y. (2009) Influence of dopant concentration on the optical properties of ZnO:In films prepared by the sol-gel method. *Thin Solid Films,* 517(17), 5023–5028. doi:10.1016/j.tsf.2009.03.037

Coates, J. (2000) Interpretation of infrared spectra: A practical approach. In R. A. Meyers (Ed.), *Encyclopedia of Analytical Chemistry* (pp. 10815–10837). John Wiley & Sons.

Dulta, K., Ağçeli, G. K., Chauhan, P., Jasrotia, R., & Chauhan, P. K. (2021) Ecofriendly synthesis of zinc oxide nanoparticles by Carica papaya leaf extract and their applications. *Journal of Cluster Science*. https://doi.org/10.1007/s10876-020-01962-w

Eslamian, M., & Shekarriz, M. (2009) Recent advances in nanoparticle preparation by spray and microemulsion methods. *Recent Patents on Nanotechnology*, 3(2), 99–115.

Fan, S. W., Srivastava, A. K., & Dravid, V. P. (2010) Nanopatterned polycrystalline ZnO for room temperature gas sensing. *Sensors and Actuators B: Chemical.* https://doi.org/10.1016/j.snb.2009.10.054

Farrokhi, M., Hosseini, S. C., Yang, J. K., & Shirzad-Siboni, M. (2014) Application of ZnO–Fe_3O_4 nanocomposite on the removal of azo dye from aqueous solutions: kinetics and equilibrium studies. *Water, Air, & Soil Pollution,* 225.

Gade, A., Ingle, A., Whiteley, C., & Rai, M. (2010) Mycogenic metal nanoparticles: progress and applications. *Biotechnology Letters*. https://doi.org/10.1007/s10529-009-0197-9

Ghorbani, H. R., Parsa Mehr, F., Pazoki, H., & Mosavar Rahmani, B. (2015) Synthesis of ZnO nanoparticles by precipitation method. *Oriental Journal of Chemistry*, 31(2), 1219–1221.

Ghazali, H.M., Mohammed, A.S. (2011) Moringa (Moringa oleifera) Seed Oil: Composition, Nutritional Aspects, and Health Attributes, *Elsevier Inc.*, 2011. doi:10.1016/B978-0-12-375688-6.10093-3.

González-Fernández, J. V., Pinzón-Moreno, D. D., Neciosup-Puican, A. A., & Carranza-Oropeza, M. V. (2021) Green method: optical and structural characterization of ZnO nanoparticles synthesized using leaf extract of Moringa oleifera. *Journal of Renewable Materials*. https://doi.org/10.32604/jrm.2021.017377

Guan, Y. F., & Pedraza, A. J. (2008) Synthesis and alignment of Zn and ZnO nanoparticles by laser-assisted chemical deposition. *Journal of Applied Physics: Nanotechnology,* 19(4), 045609. https://doi.org/10.1088/0957-4484/19/04/045609

Hadis, M., & Umit, O. (2009) ZnO Oxide: Fundamentals, Materials and Device Technology. Weinheim: *Wiley-VCH Verlag GmbH & Co*.

Hiaing, O. W. M., McCluskey, M. D., Lalonde, A. D., & Norton, M. G. (2005) Infrared spectroscopy of ZnO nanoparticles containing CO_2 impurities. *Applied Physics Letters,* 86(7), 073111.

Hong, R. Y., Qian, J. Z., & Cao, J. X. (2006) Synthesis and characterization of PMMA-grafted ZnO nanoparticles. *Powder Technology,* 163(2), 160–168.

Ider, M., Abderrafi, K., Eddahbi, A., Ouaskir, S., & Kassiba, A. (2017) Silver metallic nanoparticles with surface plasmon resonance: synthesis and characterizations. *Journal of Cluster Science*, 28, 1051–1069.

Irfan, M., Munir, H., & Ismail, H. (2021) Moringa oleifera gum-based silver and zinc oxide nanoparticles: green synthesis, characterization, and antibacterial potential against MRSA. *Biomaterials Research,* 25, 17. https://doi.org/10.1186/s40824-021-00219-7

Isnaeni, I. N., Dadan Samiarsa, D., & Primadona, I. (2021) Green synthesis of different TiO_2 nanoparticle phases using mango-peel extract. *Materials Letters*, 294, 129792.

Jafarirad, S., Mehrabi, M., Divband, B., & Kosari-Nasab, M. (2016) Biofabrication of zinc oxide nanoparticles using fruit extract of Rosa canina and their toxic potential against bacteria: a mechanistic approach. *Materials Science and Engineering*: C, 59, 296–302.

Jamil, S., Janjua, M. R. S. A., Ahmad, T., Mehmood, T., & Jing, X. (2014) Zinc oxide hollow microspheres and nanorods: synthesis and applications in gas sensors. *Materials Chemistry and Physics*, 147(1–2), 225–231.

Jayachandran, A., Aswathy, T. R., & Achuthsankar, S. N. (2021) Green synthesis and characterization of zinc oxide nanoparticles using Cayratia pedata leaf extract. *Biochemistry and Biophysics Reports*, 26, 100995. doi.org/10.1016/j.bbrep.2021.100995

Kalappurayil, T.M. & Joseph, B.P. (2016) A review of pharmacognostical studies on Moringa oleifera Lam flowers, *Pharmacogn*. J. 9, 1–7. doi.org/ 10.5530/pj.2017.1.1.

Kennedy, J., Murmu, P. P., Manikandan, E., & Lee, S. Y. (2014) Investigation of structural and photoluminescence properties of gas and metal ion-doped zinc oxide single crystals. *Journal of Alloys and Compounds*, 616, 614–617.

Liu, X., Wu, X., Cao, H., & Chang, R. P. H. (2004) Growth mechanism and properties of ZnO nanorods synthesized by plasma-enhanced chemical vapor deposition. *Journal of Applied Physics,* 95(6), 3141–3147. https://doi.org/10.1063/1.1646440

Lu, H., Zhou, Y., Vongehr, S., Tang, S., & Meng, X. (2012) Effect of hydrothermal temperature on formation and decoloration characteristics of anatase TiO_2 nanoparticles. *Science China Technological Sciences*, 55(4), 894–902.

Manguro, L.O.A. & Lemmen.P. (2007) Phenolics of Moringa oleifera leaves, *Natural product Research Former Natural Product Letters*, 21, 56- 68. doi:10.1080/1478641060105811

Manjamadha, V., & Muthukumar, K. (2016) Ultrasonic-assisted green synthesis of silver nanoparticles using a weed plant. *Biosystems Engineering,* 39, 401–411.

Minegishi, K., Koiwai, Y., Kikuchi, Y., Yano, M., Kasuga, M., & Shimizu, A. (1997) Growth of zinc oxide films by chemical vapor deposition. *Japanese Journal of Applied Physics*, 36(1), L1453–L1455. doi.org/10.1143/JJAP.36.L1453.

Nama, K.S. (2016) Moringa oleifera Lam. – Sanjana (Horseradish Tree) – a Miracle food plant with multipurpose uses in Rajasthan-India-an overview, *Int. J. Pure Appl. Biosci.* 3, 237–248, doi.org/10.18782/2320-7051.2169.

Nandiyanto, A. B. D., Oktiani, R., & Ragadhita, R. (2019) How to read and interpret FTIR spectroscopy of organic material. *Indonesian Journal of Science & Technology,* 4(1), 97–118.

Ngom, B. D., Mpahane, T., Manikandan, E., & Maaza, M. (2016) ZnO nano-discs by lyophilization process: size effects on their intrinsic luminescence. *Journal of Alloys and Compounds,* 656, 758–763.

Ngom, I., Ndiaye, N. M., Fall, A., Bakayoko, M., & Maaza, M. (2020) On the use of Moringa oleifera leaf extract for the biosynthesis of NiO and ZnO nanoparticles. *MRS Advances*. doi.org/10.1557/adv.2020.212

Ngom, I., Ngom, B.D., Sackey,J., Khamlich, S.(2020) Biosynthesis of zinc oxide nanoparticles using extracts of Moringa Oleifera: Structural & optical properties. *Materials Today: Proceedings*

Pal, S., Mondal, S., Maity, J., & Mukherjee, R. (2018) Synthesis and characterization of ZnO nanoparticles using Moringa oleifera leaf extract: investigation of photocatalytic and antibacterial activity. *International Journal of Nanoscience and Nanotechnology*, 14(2), 111–119.

Pushpamalini, T., Keerthana, M., Sangavi, R., Nagaraj, A., & Kamaraj, P. (2020). Comparative analysis of green synthesis of TiO_2 nanoparticles using four different leaf extracts. Materials Today: Proceedings.

Salavati-Niasari, M., Davar, F., & Mazaheri, M. (2008) Preparation of ZnO nanoparticles from [bis(acetylacetonato)zinc(II)]–oleylamine complex by thermal decomposition. *Materials Letters*, 62(12–13), 1890–1892.

Sharmila, G., Muthukumaran, C., Sandiya, K., Santhiya, S., Sakthi Pradeep, N., Manoj Kumar, N., Suriyanarayanan, M., & Thirumarimurugan, M. (2018) Biosynthesis, characterization, and antibacterial activity of zinc oxide nanoparticles derived from Bauhinia tomentosa leaf extract. *Journal of Nanostructure in Chemistry*, 8(3), 293–299. doi.org/10.1007/s40097-018-0271-8

Srikant, V., & Clarke, D. R. (1998) On the optical band gap of zinc oxide. *Journal of Applied Physics*, 83(10), 5447–5451. doi.org/10.1063/1.367375.

Taylor, P., Onyango, L., Manguro, A., Lemmen, P. (2007) Phenolics of Moringa oleifera leaves, Former. *Natural Product Letters* 21, 56–68. doi.org/10.1080/14786410601035811.

Udayabhanu, V., Pavitra, S. C., Sharma, S. C., & Nagaraju, G. (2019) Epigallocatechin gallate (EGCG)-assisted combustion synthesis of V_2O_5 nanoparticles for Li-ion batteries. *Ionics*. doi.org/10.1007/s11581-019-03326-5

Vafaee, M., & Ghamsari, M. S. (2007) Preparation and characterization of ZnO nanoparticles by a novel sol–gel route. *Materials Letters*, 61(14–15), 3265–3268.

Virkki, K., Tervola, E., Ince, M., Torres, T., & Tkachenko, N. V. (2018) Comparison of electron injection and recombination on TiO_2 nanoparticles and ZnO nanorods photosensitized by phthalocyanine. *Royal Society Open Science*, 5, 180323. http://dx.doi.org/10.1098/rsos.180323

Wang, Z. L. (2008) Splendid one-dimensional nanostructures of zinc oxide: a new nanomaterial family for nanotechnology. *ACS Nano*, 2(10), 1987–1992.

Xiong, G., Pal, U., Serrano, J. G., Ucer, K. B., & Williams, R. T. (2006) Photoluminescence and FTIR study of ZnO nanoparticles: the impurity and defect perspective. *Physica Status Solidi* (c), 3(10), 3577–3581.

Xu, H., Zeiger, B. W., & Suslick, K. S. (2013) Sonochemical synthesis of nanomaterials. *Chemical Society Reviews,* 42(7), 2555. https://doi.org/10.1039/c2cs35282f

Zahra, S., Bukhari, H., Qaisar, S., Sheikh, A., & Amin, A. (2022) Synthesis of nano-sized zinc oxide through an aqueous sol–gel route in polyol medium. *BMC Chemistry*, 16, 104. https://doi.org/10.1186/s13065-022-00900-3

Zhang, H., Chen, G., & Bahnemann, D. W. (2009) Photoelectrocatalytic materials for environmental applications. *Journal of Materials Chemistry*, 19(19), 5089–5121.